Characteristics of wall heat transfer from impinging diesel spray flame in low oxygen concentration ambient

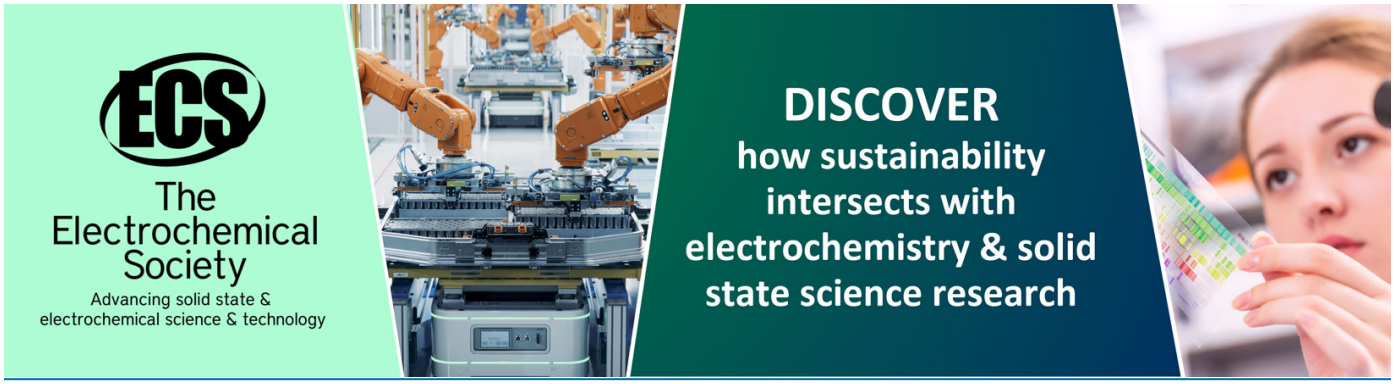

Characteristics of wall heat transfer from impinging diesel spray flame in low oxygen concentration ambient

R Mahmud[1,2], K Nishida[2], Y Ogata[2], and T Kurisu[2]

[1]Institut Teknologi Adhi Tama Surabaya, East Java, Indonesia
[2]University of Hiroshima, Japan.

rizal@itats.ac.id

Abstract. The objective of this study is to obtain an enhanced understanding of the effect of diesel spray/flame impingement on transient heat flux to the wall. By using a constant volume vessel under engine-like condition, surface heat flux of the wall at spray/flame impingement was measured with three thin film thermocouple heat flux sensors. Fuel was injected using a single-hole injector with a 0.133 mm diameter nozzle. In order to investigate the relation between diesel flame and wall heat loss, two color-method was applied to observe flame temperature distribution. 21 % and 16 % as the various oxygen concentration were investigated at each injection pressure of pressure 80, 120, and 180 MPa. The results showed that the lower oxygen concentration was generated heat loss regardless of injection pressures. The lower flame temperature and flame contact area and period were influence factor on heat loss on the wall. Furthermore, the relation between Nusselt number (*Nu*) and Reynolds number (*Re*) were also investigated to understand the heat transfer phenomena in diesel engines.

1. Introduction

In modern diesel engine, the fuel-air mixture become important factor on the combustion process and exhaust emissions, and then in thermal efficiency. In order to achieve higher efficiency of the diesel engines, it is important to improve the combustion efficiency and decrease the heat transfer through the combustion chamber wall. Therefore, fully understanding of the mechanism of heat transfer by the impinging combustion flame to the wall is required to better thermal efficiency of the diesel engines. Some studies showed that minimizing temperature difference between in-cylinder gas and combustion chamber wall surface was possible by applying insulation material such as ceramic coating on the surface [1][2]. As a result, the heat loss was reduced. Thus, both exhaust energy and piston work increased which, in turn, led to improved thermal efficiency.

Moreover, in order to reduce the emission, exhaust gas recirculation (EGR) is an effective equipment part to reduce nitrogen oxides (N_{Ox}) from diesel engines because it lowers the flame temperature and the oxygen concentration of the working fluid in the combustion chamber [3]. With increasing EGR rate, the oxygen concentration in the fuel/gas mixture decreases and the specific heat of the cylinder increases and leads reaction rate decrease. Further, in-cylinder pressure and combustion decrease [4].

In a simulation study, applying the EGR rate also considered decreasing flame temperature distribution on heat loss. Comparing the single injection results at a different EGR rate, it was confirmed that the heat flux was decreased at a higher EGR rate [5]. It was evident with an experimental study by Kuboyama [7] that the results show that EGR in a diesel engine suggests that it has the effect of reducing wall surface heat loss.

As described by the previous researchers, oxygen concentration has an effect on combustion behavior, which closely relates with lower temperature combustion. Therefore, to clarify an effect of oxygen concentration on decreasing heat loss, variation of oxygen concentration with different injection pressures will be investigated in this study. Furthermore, to investigate the relation between diesel flame and wall heat loss, two color-method was applied to observe local flame temperature distribution. Instantaneous temperature was detected by three Thin Film Thermocouple Heat Flux Sensors (TFTHFSs) which were mounted on the wall surface. By using the measured temperatures as boundary condition, we computed non-steady heat flux through the surface with finite difference method. Additionally, this research also attempts to investigate the heat transfer correlation to understand the effect of flow induced by the spray flame.

2. Experimental Set Up

2.1 High-Pressure and High-Temperature Chamber Vessel

The experiment was done same as the previously conducted one by the authors [7] using high-pressure and high-temperature chamber vessel as shown in Figure 1. It had four side windows and one of them was installed with transparent quartz windows for visualization. Two of them were provided for an injector and a spray impingement flat wall plate facing each other. In order to simulate an engine-like thermodynamic environment, pressurized hot air was supplied through an electric muffle furnace and heated with an electric heater mounted at the bottom of the chamber. The chamber pressure was manually operated, whereas the chamber temperature was controlled by a volt slider for the heater. Four K-type thermocouples were installed around the combustion area. One was fitted at a distance of 5 mm under the nozzle tip, which was placed between nozzle tip and wall, and remaining three were fitted near the wall. Diesel fuel was injected into the chamber when temperature difference of the thermocouples became within 5K. A heat flux measurement was done a little later after hot gas feed for avoiding turbulence in the vessel.

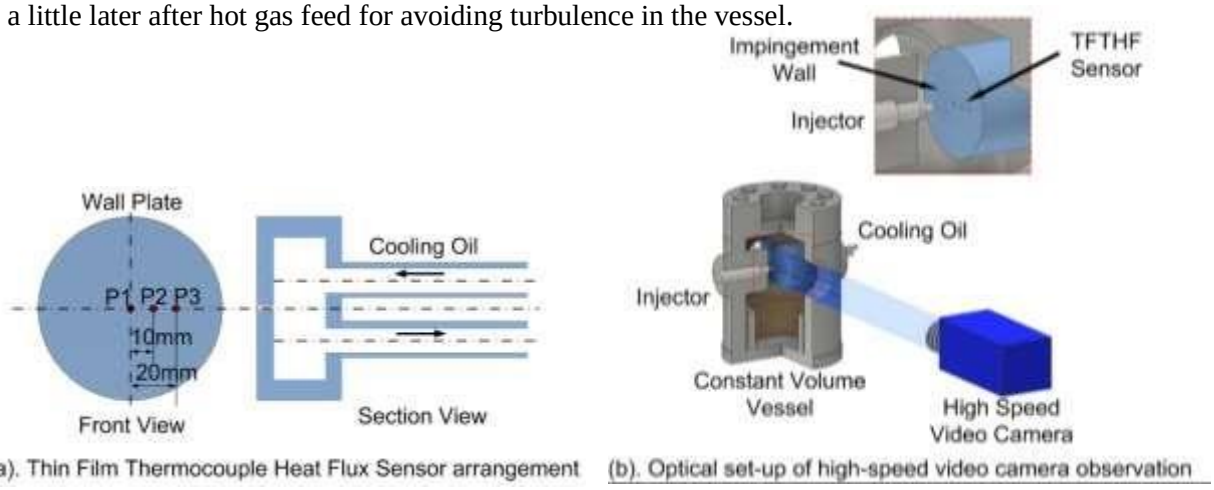

Figure 1. Thin Film Thermocouple Heat Flux Sensor arrangement and optical set-up of high-speed video camera observation

The flat wall was made of stainless steel which has a thickness of 7.3 mm. The back side of the wall plate was cooled by oil in order to form one-directional heat flow across the wall as shown in Figure 1 (a). The cooling oil temperature was kept constant by a thermostatic oil bath. Three micro

heat flux sensors were mounted on the impinging surface side of the wall by means of high-temperature adhesive as shown in Figure 1 (b). Fuel, which was supplied from a common rail system, was injected through a single hole nozzle injector controlled by an Electronic Control Unit (ECU). Injection quantity and timing was controlled by a delay pulse generator (Stanford Research Systems DG645). Injection pulse had been calibrated by the injection rate measurement previously.

2.2 Heat Flux and Total Heat Loss Measurement

To obtain the instantaneous surface heat flux on the wall, three Alumel/Chromel TFTHFSs (Medtherm 10702B) were applied as shown in Figure 1 (a). The sensor consists of two thermocouple sensors. One is a surface temperature sensor and the other is an inner temperature sensor. Diameter of the sensors is ø 1.55 mm, and distance between it's thermal contacts (surface and inside) is 3.30 mm. The sensors were radially located on the wall surface with a 10 mm distance each other. Positions of the sensors are designated as Position1 (center of wall impingement), Position2 (10 mm from center) and Position3 (20 mm from center) Instantaneous local heat flux was computed by applying one- dimensional non-steady heat conduction equation using two measured temperatures by the identical sensor as boundary conditions. Steady component of the heat flux, however, was neglected. The equation was explained in the previous report [8].

Table.1 Experimental conditions

Ambient Condition	
Ambient gas	Air (N_2: 79%, O_2: 21%), (N_2: 84%, O_2: 16%)
Ambient pressure (MPa)	4.1
Ambient temperature (K)	873
Ambient density (kg/m³)	16
Injection Condition	
Fuel	Diesel fuel
Injector type	Piezo actuator type
Number of nozzle holes	1
Injection quantity (mm³)	5
Diameter of nozzle hole (mm)	0.133
Injection pressure (MPa)	80, 120, 180
Impingement Condition	
Impingement wall	Flat plate, Stainless steel
Impingement distance (mm)	40
Wall temperature (K)	460 ±10
Cooling method	Oil cooling

Total heat loss was calculated by integrating the heat flux with concentric area and time. In area integration, heat flux affecting areas were defined as concentric circles of 0-5 mm for Area 1, 5-15 mm for Area 2, and 15-25 mm for Area 3, respectively as shown in Figure 2.

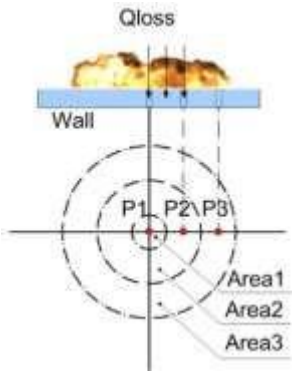

Figure 2. Areas at wall surface

2.3 High-Speed Video Camera Observation

Figure 1 (b) shows optical set-up of high-speed video camera observation and it's arrangement. The camera (Nac Image Technology Inc, HX-3) was utilized to record the flame behavior with an imaging speed of 20,000 fps and resolution of 320 x 448 pixels. Observation of flame was conducted with natural flame luminosity. Moreover, in order to investigate the mechanism of diesel flame and the wall heat loss, the two-color method was used to observe flame temperature distribution from luminous flame. We used a two-color pyrometry software named "Thermias" of Nac Company for analyzing the natural flame color images. A standard light illuminant was used for calibration of it.

2.4. Test Conditions

Experimental measurement conditions are listed in Table 1. It was decided based on actual operation of small size diesel engines. In order to self-ignite the fuel, pressure and temperature were set at those of compression TDC (top dead center) in low load operation for the combustion test. Injection quantity was 5 mm^3 using 0.133 mm nozzle hole diameter. The impinging distance between the nozzle tip to the impingement wall was set at 40 mm. Oxygen concentrations were conducted at 21% and 16% as experimental parameters to investigate the effect of the heat transfer characteristics on the impinging flame on the wall. The all oxygen concentration tests were conducted at three injection pressures, i.e. 80, 120, and 180 MPa. The conditions was set combusting spray at high temperature and high pressure ambient. The gas density is 16 kg/m^3 with 4.1 MPa ambient pressure.

3. Results and Discussion

3.1 Wall Heat Transfer

In this section, effects of the oxygen concentration and injection pressure on wall heat transfer were investigated. Figure 3 presents the combined effect of oxygen concentration/injection pressure on the transferred heat and ratio of heat loss to the total combustion heat. 21 and 16 % as the various oxygen concentration were investigated at each injection pressure of pressure 80, 120, and 180 MPa. The combined effect can be explained as follows:

Firstly, the heat transferred increased gradually with increasing injection pressure at O_2 = 21 %. However, it was not applied to O_2 = 16 %, the heat transferred increased disproportionately even though the injection pressure was increased. It means high velocity by increasing injection pressure was not dominant factor on transferred heat when oxygen concentration under 21 %. Secondly, lower oxygen concentrations consistently reduce heat transfer on the wall in all conditions. This decreased due to the flame temperature was lower. It can be proved by the flame temperature distribution that will be explained in the next section. By higher oxygen concentration as 21 %, it allows more stable combustion with produce high flame temperature then can lead more rate of heat transfer. And then thirdly, the ratio of heat loss through the wall accounts for about 10-15 % of total combustion energy.

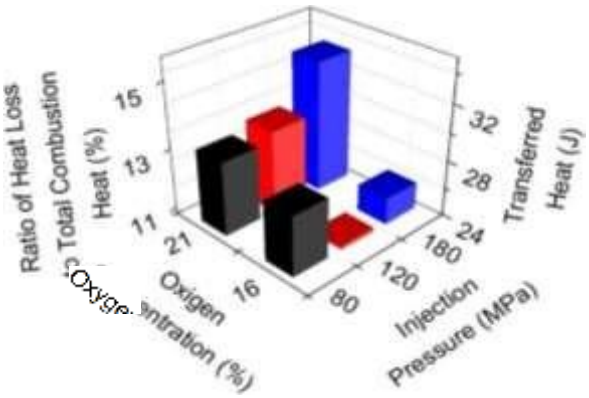

Figure 3. Transferred heat at different oxygen concentration and injection pressure

Considering Figure 3, at lower oxygen concentration, the transferred heat decreased even though injection pressure was increase. It is inversely proportional when oxygen concentration was set O_2 = 21 %. Therefore, the studied will be focus on effect of oxygen concentration, i.e. O_2 = 21 % and O_2 = 16 % at 120 MPa injection pressure. Then, proceed to discuss the following combination of oxygen concentration and injection pressure, i.e. O_2/P_{inj} = 16/80, 16/180 and 21/180 (%/MPa) each. These conditions can represent both comparison different effect of injection pressures and oxygen concentration.

3.2 Heat Flux on the Wall Surface at different Oxygen Concentration

Non-steady local heat fluxes with flame impinging on the wall and integrated luminosity from flame images at different oxygen concentrations are presented in Figure 4 (a-b). The figure shows a significant difference in the ignition timing both conditions. The low temperature due to decreasing oxygen concentration causes unsuitable equivalence ratio for ignition. As a result, local heat flux at Position 1 and 2 started to increase earlier before the ignition occurred. The most surprising is the peak value of local heat flux was dramatically decreased when the ignition occurred later after spray impingement. It is because the both positions increased mainly by convective evaporation spray during the injection duration. Consequently, the rate of heat transfer was lower around area Position1 and 2. However, in case of O_2 = 21 %, the ignition occurred just after impingement in which cover Position1 and 2, as a result Position2 increased simultaneously with ignition and gave substantial amount on local heat flux in that region. The temperature distribution also playing role on this phenomenon.

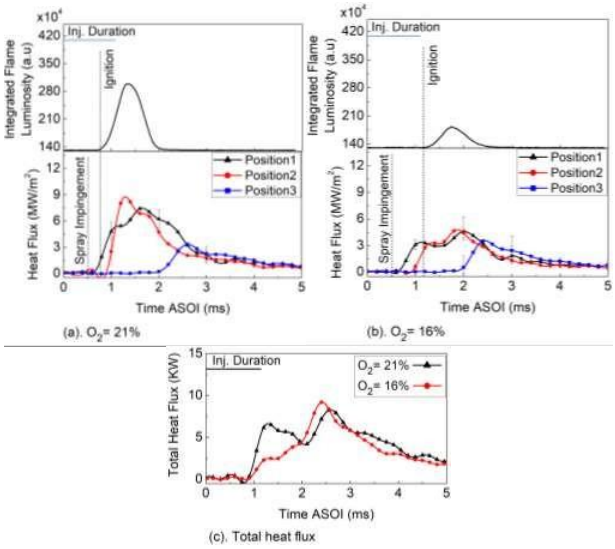

Figure 4. Temporal variation of local heat flux, integrated flame luminosity, and total heat flux at different oxygen concentration

Even though, local heat flux increase and higher peak value was observed at Position1 and 2 under O_2 = 21 %. However, there was no significant difference in Position3 at both conditions. The wall friction and momentum loss due to turbulent mixing took place at Position3 as the far area from the center of impingement.

Figure 4 (c) shows temporal variation of the total heat flux at different oxygen concentrations. It can be seen in the graph, O_2 of 21 % had two peaks waves i.e. there were two stages for the local heat transfer. At first, the local heat flux was increased by turbulence of impingement spray and thereafter when the flame contacts the wall, it develops to a circular area where the flame velocity decreases due to the fact that effects of wall friction takes place, then heat transfer occurs. While O_2 of 16 % accumulated at the second stage for local heat transfer due to significant ignition delay. Consequently, the temperature distribution was appeared far away from the center of impingement in which influence on larger area.

3.3 Flame Natural Luminosity and Flame Temperature

In this section, impinging flame behavior under oxygen concentration are studied. Effects of the oxygen concentrations (O_2), which 21 and 16 % were investigated at impingement distance of 40 mm. Figure 5 shows images of impinging flame natural luminosity at different oxygen concentrations. In this Figure, the luminous flame appeared earlier with O_2 = 21 %. It had started at 0.9 ms ASOI (after start of injection) before the end of injection (EOI) and at 1.25 ms ASOI just after the EOI for O_2 = 16 %. It is found that the reduction of the oxygen concentration in the enclosure mainly affects the

reactions in the gas phase and results in changes of the combustion behavior such as ignition timing and flame development. It can be seen at 1.5 to 1.8 ms ASOI, flame natural luminosity start to be decreased at O_2 = 21 %. However, it starts to develop at O_2 = 16 % due to ignition delay was decrease. Consideration the intensity of luminous flame, they were surprisingly different each other. As shown in the figure, lower oxygen concentration generated lower luminous and flame develops quite slowly. Oxygen concentration is therefore required to complete the combustion process since the ignition was not possible occurred without any oxygen.

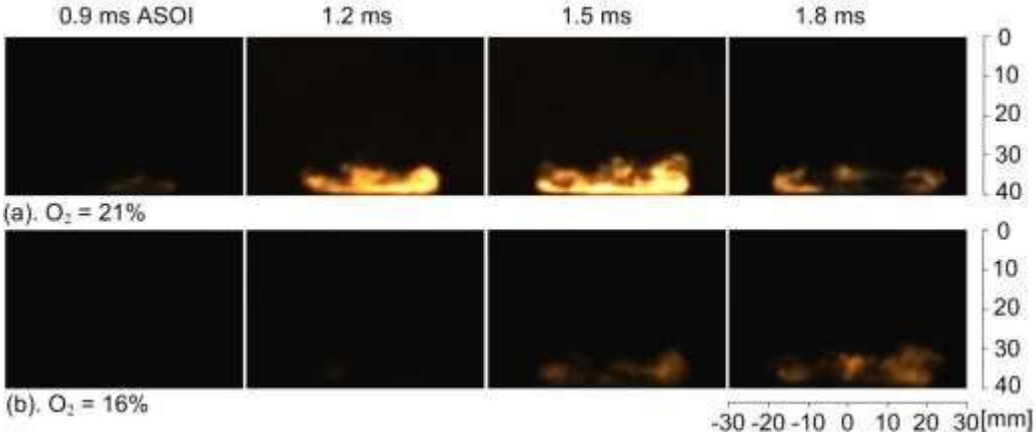

Figure 5. Flame natural luminosity at different oxygen concentration

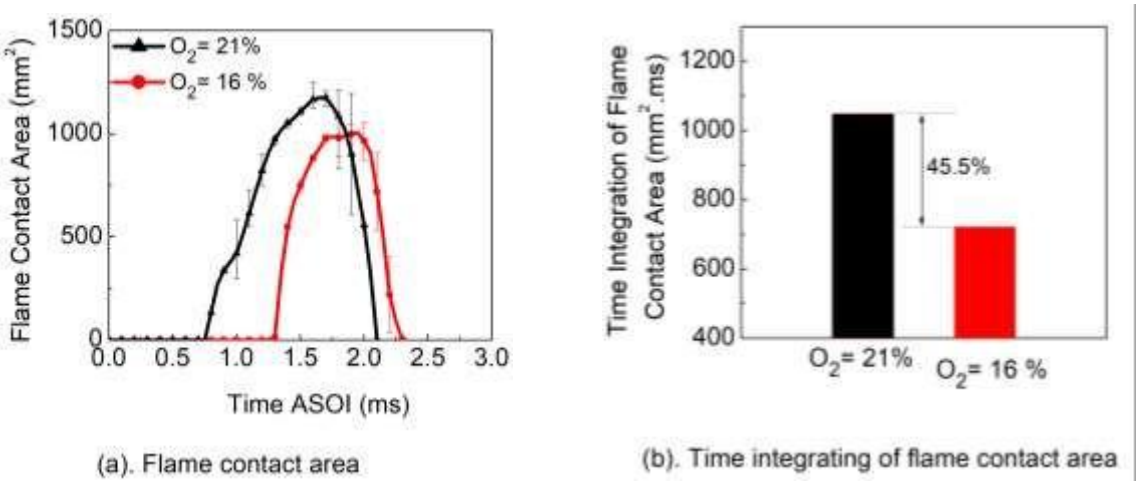

Figure 6. Comparison of flame contact area and time integrating of flame contact area at different oxygen concentration

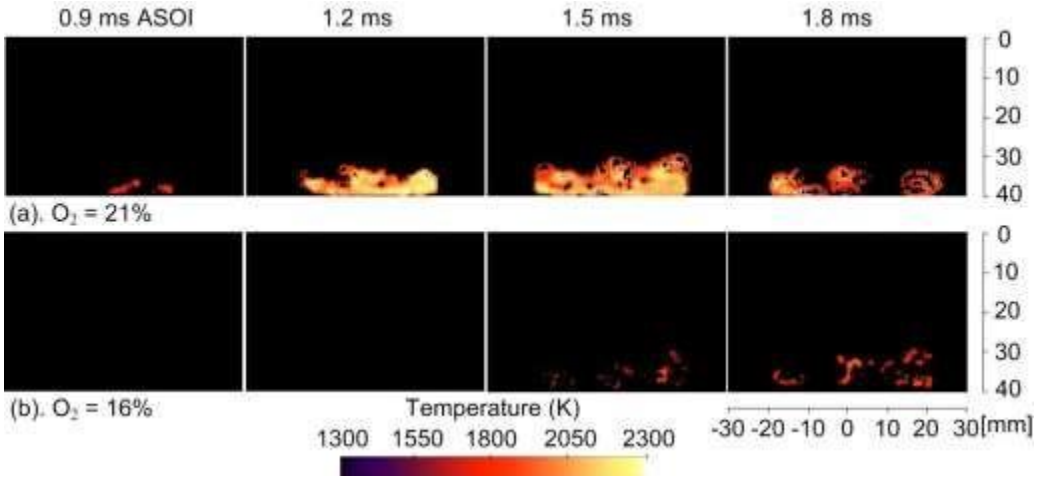

Figure 7. Flame temperature distribution at different oxygen concentration

Effect of flame contact to the wall at different oxygen concentrations are presented in Figure 6. Figure 6 (a) shows that O_2 =16 % had smaller contact area than that O_2 =21 %. It means with oxygen concentration of 21 %, leads to flame contact significantly to spread wide into circumferential area of flat wall. This flame contact area contributes to the heat transfer by conduction. The larger flame contact area causes larger area to be affected to rate of heat transfer. Time integration of the flame contact area can be seen in Figure 6 (b), which shows that flame traveling distance was shorter as the oxygen concentration is decreased.

Figure 7 shows flame temperature distributions at different oxygen concentrations obtained from two-color method analysis, which was performed with flame natural luminosity images. By comparing the temperature distributions with different oxygen concentrations, it can be seen that the temperature distribution was decreased by decreasing oxygen concentration. It can be inferred from Figure 8 that burned gas temperature decreases with decreasing volume fraction of oxygen because the heat capacity of ambient gas increase with decreasing the volume oxygen concentration [8]. When the combustion temperature was low, the temperature difference between the flame and the wall surface were decreased. So that it will have an impact on the reduced energy lost to the wall. Decreasing oxygen concentration was effective parameter for reducing the heat transfer on the wall. Furthermore, soot emission during combustion process also decreased at low temperature as can be seen that the luminous flame significantly decreased. At O_2 = 16 %, the maximum temperature was 1785 K, around 400 K decreased from the peak value of O_2 = 21 %.

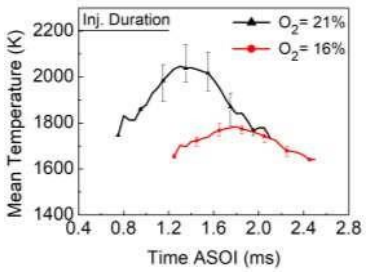

Figure 8. Mean temperature at different oxygen concentration

3.4 Heat Flux on the Wall Surface at Different Oxygen Concentration and Injection Pressure

Non-steady local heat flux and integrated luminosity with the combination of oxygen concentration and injection pressure (O_2/P_{inj}) conditions are presented in Figure 9 (a-c). Figure 9 (a-b) demonstrates the comparison of injection pressure in the combined effect. In the previous report [9], effect of injection pressure was explained in detail. However, since the oxygen concentration of 16 % produced lower flame temperature, it is interesting to clarify the phenomenon in local heat flux history. By comparing the combination of O_2/P_{inj} = 16/80 and 16/180 as shown in the Figure 9 (a-b), local heat flux waveform at all positions started to increase earlier at combination of O_2/P_{inj} = 16/180. It is certainly due to increasing injection pressure related to increasing velocity. On the other hand, local heat flux peak value was almost similar in these combinations. Regarding this phenomenon, increasing injection pressure did not affect more on local heat flux at oxygen concentration of 16 % due to both temperatures are lower. Even though spray mixture increases by higher injection pressure, the time of ignition was not change with pressure, but the combustion process was significant decreased in this condition. At lower injection pressure, combustion duration is slightly longer which causes the flame contact was stayed longer on the wall. As a result, transferred heat to the wall increased as shown in Figure 3.

Figure 9 (b-c) shows a comparison of oxygen concentration in the combined effect. Combination of O_2/P_{inj} = 21/180 had high local heat flux at all positions. With the increased oxygen concentration, increased both the fuel-air mixture and the reaction rate. As a result, the flame temperature increased and this flame gas flow distributed along the wall due to high injection pressure, then lead the increase rate of the heat transfer. However, at lower oxygen concentration, the heat loss was decreased. It is due to the lower flame temperature and the reduced area contact period between the flame and the wall surface as shown in Figure 10 (b), caused by the higher heat capacity and density of the ambient gas [10].

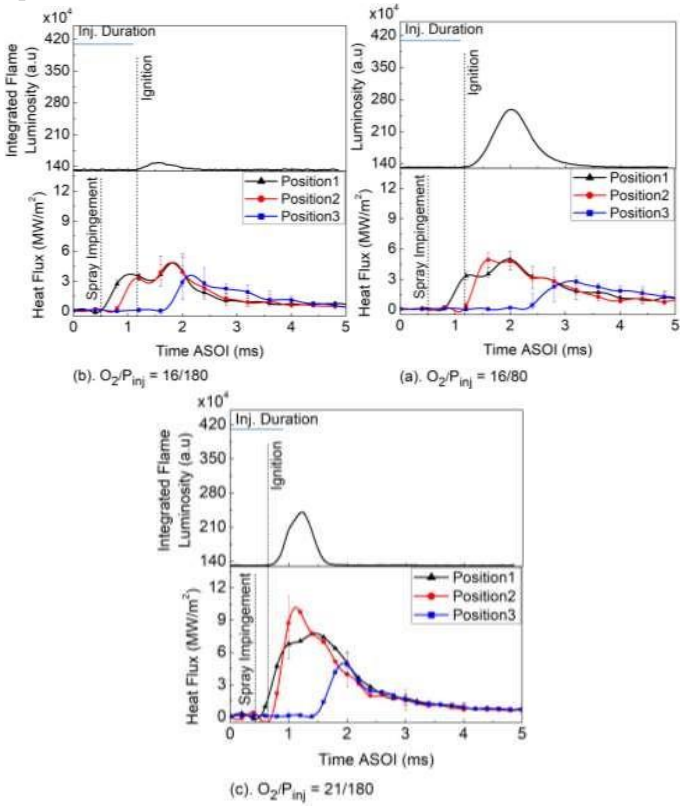

Figure 9. Temporal variation of local heat flux, integrated flame luminosity, and total heat flux at different oxygen concentration and injection pressure

Temporal changes of the flame contact area and time integrating of flame contact area at the different oxygen concentration and injection pressure are shown in Figure 10 (a-b). It shows that combination of O_2/P_{inj} = 16/80 and 16/180 makes flame contact area to increase later comparing O_2/P_{inj}
= 21/180. As mentioned in the previous section that oxygen concentration of 16 % lead ignition occur later after spray impingement on the wall as shown in Figure 5. Comparing three combinations, O_2/P_{inj}
= 16/180 have a smaller flame contact area and shorter resident time flame contact on the wall as shown in Figure 10 (b).

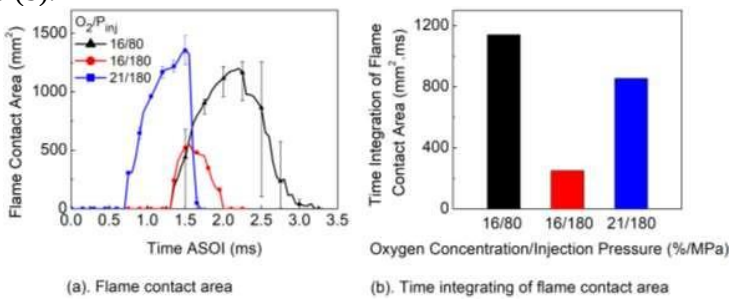

Figure 10. Comparison of flame contact area and time integrating of flame contact area at different oxygen concentration and injection pressure

3.5 Nusselt-Reynold Number Analysis

According to the influence of different injection pressure, the spray flame flow has considerable effect on heat loss through the wall. Then, we studied relation between Reynold number (*Re*) and Nusselt number (*Nu*). The basis of these correlations has relied on dimensional analysis for turbulent flow that corelates the Nusselt (*Nu*), Reynolds (*Re*), and Prandtl (*Pr*) numbers as shown equation (1). The relationship among *Nu, Re,* and *Pr* numbers, which follow those found applied in a turbulent heat transfer equation of the pipe's internal flow or over flat plates [11],[12].

$$Nu = (Const)\ x\ Re^m x\ Pr^n \tag{1}$$

$$Nu = \frac{h.L}{\lambda} \tag{2}$$

$$Re = \frac{\rho.U.L}{\mu} \tag{3}$$

$$Pr = \frac{\mu.cp}{\lambda} \tag{4}$$

Where *Nu, Re* and *Pr* are difined as the following equation (2), (3), and (4). m and n are defined based on the laminar or turbulent heat transfer. H is heat transfer coefficient, L is characteristic length, λ is thermal conductivity, ρ is density, *U* is characteristic velocity at each position, μ is viscosity and *cp* is specific heat. We used distance between the nozzle tip and the wall as the characteristic length.

As shown in equation (3), Re number requires characteristic flow velocity. As characteristics velocity, mean piston speed is usually used in previously proposed heat transfer equations. In this study, we utilized waveforms of the heat flux as represented characteristics velocity. In order to investigate characteristic flow velocity, flamelet velocity determined according to local combustion flame motion near wall which has direct impact on local heat flux waveform characteristic. It was assumed that the waveform which had clear peaks as a consequence of combustion flame motion. The calculation method of flamelet velocity was explained in detail in the previous report [10].

Figure 11 performing a correlation between *Re* and *Nu* number at difference of oxygen concentrations and injection pressures. For *Re* number calculation, impingement distance is selected as a representative length, i.e. 40 mm. For *Nu* number calculation, thermodynamic properties of air were taken into account. It can be seen from the figure, the *Nu* number was proportional to *Re* number at all conditions. High turbulence flow from combustion which is characterized by high Reynolds number is one of the major factors causing a large amount of heat transfer on the wall.

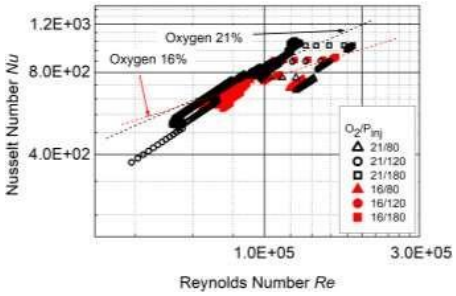

Figure 11. Correlation between Reynolds number and Nusselt number at oxygen concentration/injection pressure.

4. Conclusions

Effects of oxygen concentration and injection pressure on the combustion wall heat transfer under diesel engine-like conditions were investigated. The main conclusions are summarized as follows: By comparing the temperature distributions with different oxygen concentrations, it was found that the temperature distribution and flame contact area were decreased with a decreasing oxygen concentration. When the combustion temperature was low, the temperature difference between the flame and wall surface was smaller. As a result, the local heat flux decreased, and the transferred heat value was also reduced. Under the combined effects of the oxygen concentration and injection pressure, lower oxygen concentrations were consistently reduced the heat transfer on the wall in all conditions. The transferred heat decreased even when the injection pressure was increased. This occurred because the flame temperature was lower compared with the base oxygen concentration of O2 = 21 %. In this study, using the flamelet velocity value, it was found that the *Nu* number was proportional to the *Re* number. Its mean, value of *Nu* number is high when the *Re* number value increased.

Nomenclatures

EGR	: Exhaust Gas Circulation
N_{ox}	: Nitrogen Oxides
TFTHFS	: Thin Film Thermocouple Heat Flux Sensor
ASOI	: After Start of Injection
O_2	: Oxygen Concentration
a.u.	: arbitrary units
Nu	: Nusselt Number
Re	: Reynolds Number
Pr	: Prandtl Number

5. References

[1] T. Kogo, Y. Hamamura, K. Nakatani, T. Toda, A. Kawaguchi, and A. Shoji, ―High Efficiency Diesel Engine with Low Heat Loss Combustion Concept - Toyota's Inline 4-Cylinder 2.8-Liter ESTEC 1GD-FTV Engine - Toyota's i,‖ in SAE Technical Papers, Apr. 2016, vol. 2016-April, no. April, doi: 10.4271/2016-01-0658.

[2] K. Fukui, Y. Wakisaka, K. Nishikawa, Y. Hattori, H. Kosaka, and A. Kawaguchi,

―Development of Instantaneous Temperature Measurement Technique for Combustion Chamber Surface and Verification of Temperature Swing Concept,‖ Apr. 2016, doi: 10.4271/2016-01-0675.

[3] M. Zheng, G. T. Reader, and J. G. Hawley, ―Diesel engine exhaust gas recirculation - A review on advanced and novel concepts,‖ Energy Convers. Manag., vol. 45, no. 6, pp. 883–900, 2004, doi: 10.1016/S0196-8904(03)00194-8.

[4] X. Cheng, L. Chen, F. Yan, G. Hong, Y. Yin, and H. Liu, ―Investigations of Split Injection Strategies for the Improvement of Combustion and Soot Emissions Chraracteristics Baesed on the Two-Color Method in a Heavy-Duty Diesel Engine,‖ SAE Tech. Pap. 2013-01-2523., 2013.

[5] H. Osada, N. Uchida, K. Shimada, and Y. Aoyagi, ―Reexamination of Multiple Fuel Injections for Improving the Thermal Efficiency of a Heavy-Duty Diesel Engine,‖ SAE Tech. Pap. 2013- 01-0909, 2013, doi: 10.4271/2013-01-0909.

[6] T. Kuboyama and H. Kosaka, ―A Measurement of Heat loss in Combustion Chamber of DI Diesel Engines,‖ Marit. Res. Inst. Technol. Saf., vol. 8, no. 215–221, pp. 89–96, 2008.

[7] R. Mahmud, T. Kurisu, K. Nishida, Y. Ogata, J. Kanzaki, and T. Tadokoro, ―Experimental study on flat-wall impinging spray flame and its heat flux on wall under diesel engine–like condition: First report—effect of impingement distance,‖ Proc. Inst. Mech. Eng. Part D J. Automob. Eng., vol. 233, no. 8, pp. 2187–2202, Jul. 2019, doi: 10.1177/0954407018778153.

[8] T. Kuboyama and Y. Moriyoshi, ―Heat Transfer Analysis in a Diesel Engine Based on a Heat Flux Measurement using a Rapid Compression and Expansion Machine,‖ SAE Tech. Pap. 2017-32-0115, p. 6, 2017.

[9] R. Mahmud, T. Kurisu, K. Nishida, Y. Ogata, J. Kanzaki, and O. Akgol, ―Effects of injection pressure and impingement distance on flat-wall impinging spray flame and its heat flux under diesel engine-like condition,‖ Adv. Mech. Eng., vol. 11, no. 7, p. 168781401986291, Jul. 2019, doi: 10.1177/1687814019862910.

[10] T. KUBOYAMA, H. KOSAKA, T. AIZAWA, and Y. MATSUI, ―A Study on Heat Loss in DI Diesel Engines by Using a Rapid Compression and Expansion Machine (1st Report, The Effects of Oxygen Volume Fraction and Density of Ambient Gas on Heat Loss),‖ Japan Soc. Mech. Eng., vol. 72, no. 721, pp. 2315–2322, 2006.

[11] J. P. Holman et al., ―McGraw-Hill Series in Mechanical Engineering INTERNAL COMBUSTION ENGINE Xnderung nur iiber,‖ 1988.

[12] J. Chang et al., ―New Heat transfer Correlation for an HCCI Engine Derived from Measurements of Instantaneous Surface Heat Flux,‖ SAE,‖ 2004,. [Online]. Available: https://citeseerx.ist.psu.edu/viewdoc/summary?doi=10.1.1.473.5101.

Acknowledgements

We would like to thank Mazda Motor Corporation for their support with measurement in this study.